

Local field dynamics in symmetric Q -Ising neural networks

D. Bollé ^{*†}

Instituut voor Theoretische Fysica, K.U. Leuven,
B-3001 Leuven, Belgium

and G. M. Shim [‡]

Department of Physics, Chungnam National University
Yuseong, Taejon 305-764, R.O. Korea

Abstract

The time evolution of the local field in *symmetric* Q -Ising neural networks is studied for arbitrary Q . In particular, the structure of the noise and the appearance of gaps in the probability distribution are discussed. Results are presented for several values of Q and compared with numerical simulations.

Key words: Symmetric networks; Q -Ising neurons; parallel dynamics; local field; probabilistic approach

*e-mail: desire.bolle@fys.kuleuven.ac.be.

†Also at Interdisciplinair Centrum voor Neurale Netwerken, K.U.Leuven, Belgium.

‡e-mail: gmshim@cnu.ac.kr.

1 Introduction

In a number of papers in the nineties (cfr. [1]-[10] and references therein) the parallel dynamics of Q -Ising type neural networks has been discussed for several architectures –extremely diluted, layered feedforward, recurrent– using a probabilistic approach. For the asymmetric extremely diluted and layered architectures the dynamics can be solved exactly and it is known that the local field only contains Gaussian noise. For networks with symmetric connections, however, things are quite different. Even for extremely diluted versions of these systems feedback correlations become essential from the second time step onwards, complicating the dynamics in a nontrivial way.

A complete solution for the parallel dynamics of symmetric Q -Ising networks at zero-temperature taking into account all feedback correlations, has been obtained only recently using a probabilistic signal-to-noise ratio analysis [9]-[10]. Thereby it is seen that both for the fully connected and the extremely diluted symmetric architectures, the local field contains a discrete and a normally distributed noise part. The difference between the two architectures is that for the diluted model the discrete part at a certain time t does not involve the spins at all previous times $t-1, t-2, \dots$ up to 0 but only the spins at time step $t-1$. Even so, this discrete part prevents a closed-form solution of the dynamics but a recursive scheme can be developed in order to calculate the complete time evolution of the order parameters, i.e., the retrieval overlap and the activity.

In the work above the focus has been on the non-equilibrium behavior of the order parameters of the network. But, since the local field itself is a basic ingredient in the development of the relevant recursive scheme it is interesting to study also the non-equilibrium behavior of the local field distribution. The more so since this distribution does not convergence to a simple sum of Gaussians as is frequently thought, but it develops a gap structure. This is precisely one of the points studied in detail in the present communication. Moreover, the analogies and differences between the fully connected architecture and the symmetrically diluted one are highlighted. Finally, numerical simulations are presented confirming the analytic study and giving additional insight in the structure of these local field distributions.

2 The model

Consider a neural network Λ consisting of N neurons which can take values σ_i from a discrete set $\mathcal{S} = \{-1 = s_1 < s_2 < \dots < s_Q = +1\}$. The p patterns

to be stored in this network are supposed to be a collection of independent and identically distributed random variables (i.i.d.r.v.), $\{\xi_i^\mu \in \mathcal{S}\}$, $\mu \in \mathcal{P} = \{1, \dots, p\}$ and $i \in \Lambda$, with zero mean, $E[\xi_i^\mu] = 0$, and variance $A = \text{Var}[\xi_i^\mu]$. The latter is a measure for the activity of the patterns. Given the configuration $\sigma_\Lambda(t) \equiv \{\sigma_j(t)\}$, $j \in \Lambda = \{1, \dots, N\}$, the local field in neuron i equals

$$h_i(\sigma_\Lambda(t)) = \sum_{j \in \Lambda} J_{ij}(t) \sigma_j(t) \quad (1)$$

with J_{ij} the synaptic coupling from neuron j to neuron i . In the sequel we write the shorthand notation $h_{\Lambda,i}(t) \equiv h_i(\sigma_\Lambda(t))$.

For the extremely diluted symmetric (SED) and the fully connected (FC) architectures the couplings are given by the Hebb rule

$$J_{ij}^{SED} = \frac{c_{ij}}{CA} \sum_{\mu \in \mathcal{P}} \xi_i^\mu \xi_j^\mu \quad \text{for } i \neq j, \quad J_{ii}^{SED} = 0, \quad (2)$$

$$J_{ij}^{FC} = \frac{1}{NA} \sum_{\mu \in \mathcal{P}} \xi_i^\mu \xi_j^\mu \quad \text{for } i \neq j, \quad J_{ii}^{FC} = 0, \quad (3)$$

with the $\{c_{ij} = 0, 1\}$, $i, j \in \Lambda$ chosen to be i.i.d.r.v. with distribution $\text{Pr}\{c_{ij} = x\} = (1 - C/N)\delta_{x,0} + (C/N)\delta_{x,1}$ and satisfying $c_{ij} = c_{ji}$.

For the diluted symmetric model the architecture is a local Cayley-tree but, in contrast with the diluted asymmetric model, it is no longer directed such that it causes a feedback from $t \geq 2$ onwards. In the limit $N \rightarrow \infty$ the probability that the number of connections $T_i = \{j \in \Lambda | c_{ij} = 1\}$ giving information to the site $i \in \Lambda$, is still a Poisson distribution with mean $C = E[|T_i|]$. Thereby it is assumed that $C \ll \log N$ and in order to get an infinite average connectivity allowing to store infinitely many patterns one also takes the limit $C \rightarrow \infty$ [10].

At zero temperature all neurons are updated in parallel according to the rule

$$\begin{aligned} \sigma_i(t+1) &= g_b(h_{\Lambda,i}(t)) \\ g_b(x) &\equiv \sum_{k=1}^Q s_k [\theta [b(s_{k+1} + s_k) - x] - \theta [b(s_k + s_{k-1}) - x]] \end{aligned} \quad (4)$$

with $s_0 \equiv -\infty$ and $s_{Q+1} \equiv +\infty$. Here $g_b(\cdot)$ is the gain function and $b > 0$ is the gain parameter of the system. For finite Q , this gain function is a step function. The gain parameter b controls the average slope of $g_b(\cdot)$.

3 Local field dynamics

In order to measure the retrieval quality of the system one can use the Hamming distance between a stored pattern and the microscopic state of the network

$$d(\boldsymbol{\xi}^\mu, \boldsymbol{\sigma}_\Lambda(t)) \equiv \frac{1}{N} \sum_{i \in \Lambda} [\xi_i^\mu - \sigma_i(t)]^2. \quad (5)$$

This introduces the main overlap and the arithmetic mean of the neuron activities

$$m_\Lambda^\mu(t) = \frac{1}{NA} \sum_{i \in \Lambda} \xi_i^\mu \sigma_i(t), \quad \mu \in \mathcal{P}; \quad a_\Lambda(t) = \frac{1}{N} \sum_{i \in \Lambda} [\sigma_i(t)]^2. \quad (6)$$

The key question is then how these quantities evolve in time under the parallel dynamics specified before. For a general time step we find from eq. (4) using the law of large numbers (LLN) that in the thermodynamic limit

$$m^1(t+1) \stackrel{Pr}{\equiv} \frac{1}{A} \langle\langle \xi_i^1 g_b(h_i(t)) \rangle\rangle, \quad a(t+1) \stackrel{Pr}{\equiv} \langle\langle g_b^2(h_i(t)) \rangle\rangle, \quad (7)$$

where the convergence is in probability [11]. In the above $\langle\langle \cdot \rangle\rangle$ denotes the average both over the distribution of the embedded patterns $\{\xi_i^\mu\}$ and the initial configurations $\{\sigma_i(0)\}$. The average over the latter is hidden in an average over the local field through the updating rule (4).

Some remarks are in order. For the symmetric diluted model the sum over the sites i is restricted to T_j , the part of the tree connected to neuron j . Moreover, for that model the thermodynamic limit contains the limit $C \rightarrow \infty$ besides the $N \rightarrow \infty$ limit. In this thermodynamic limit $C, N \rightarrow \infty$ all averages have to be taken over the treelike structure, viz. $\frac{1}{N} \sum_{i \in \Lambda} \rightarrow \frac{1}{C} \sum_{i \in T_j}$, and the capacity defined by $\alpha = p/N$ has to be replaced by $\alpha = p/C$.

In (7) the local field is the main ingredient. Suppose that the initial configuration of the network $\{\sigma_i(0)\}, i \in \Lambda$, is a collection of i.i.d.r.v. with mean $E[\sigma_i(0)] = 0$, variance $\text{Var}[\sigma_i(0)] = a_0$, and correlated with only one stored pattern, say the first one $\{\xi_i^1\}$:

$$E[\xi_i^\mu \sigma_j(0)] = \delta_{i,j} \delta_{\mu,1} m_0^1 A \quad (8)$$

with $m_0^1 > 0$. By the LLN one gets for the main overlap and the activity at $t = 0$

$$m^1(0) \equiv \lim_{(C), N \rightarrow \infty} m_\Lambda^1(0) \stackrel{Pr}{\equiv} \frac{1}{A} E[\xi_i^1 \sigma_i(0)] = m_0^1 \quad (9)$$

$$a(0) \equiv \lim_{(C), N \rightarrow \infty} a_\Lambda(0) \stackrel{Pr}{\equiv} E[\sigma_i^2(0)] = a_0 \quad (10)$$

where the notation should be clear. In order to obtain the configuration at $t = 1$ we have to calculate the local field (1) at $t = 0$. To do this we employ the probabilistic signal-to-noise ratio analysis ([1]-[10]). Recalling the learning rule (3) we separate the part containing the signal from the part containing the noise. In the limit $N \rightarrow \infty$ we then arrive at

$$h_i(0) \equiv \lim_{N \rightarrow \infty} h_{\Lambda,i}(0) \stackrel{\mathcal{D}}{=} \xi_i^1 m^1(0) + \mathcal{N}(0, \alpha a(0)) \quad (11)$$

where the convergence is in distribution [11] and with $\mathcal{N}(0, V)$ representing a Gaussian random variable with mean 0 and variance V . We note that this structure of the distribution of the local field at time zero – signal plus Gaussian noise – is typical for all architectures treated in the literature.

For a general time step $t + 1$, a tedious study reveals that the distribution of the local field is given by [9], [10]

$$h_i(t+1) = \xi_i^1 m^1(t+1) + \mathcal{N}(0, \alpha a(t+1)) + \chi(t)[F(h_i(t) - \xi_i^1 m^1(t)) + \alpha \sigma_i(t)] \quad (12)$$

where $F = 1$ for the fully connected architecture and $F = 0$ for the symmetrically diluted one. So, the local field at time t consists out of a discrete part and a normally distributed part, viz.

$$h_i(t) = M_i(t) + \mathcal{N}(0, V(t)) \quad (13)$$

where $M_i(t)$ and $V(t)$ satisfy the recursion relations

$$M_i(t+1) = \chi(t)[F(M_i(t) - \xi_i^1 m^1(t)) + \alpha \sigma_i(t)] + \xi_i^1 m^1(t+1) \quad (14)$$

$$V(t+1) = \alpha a(t+1)A + F\chi^2(t)V(t) + 2F\alpha A\chi(t)\text{Cov}[\tilde{r}^\mu(t), r^\mu(t)]. \quad (15)$$

The quantity $\chi(t)$ reads

$$\chi(t) = \sum_{k=1}^{Q-1} f_{h_i^\mu(t)}(b(s_{k+1} + s_k))(s_{k+1} - s_k) \quad (16)$$

where $f_{h_i^\mu(t)}$ is the probability density of $h_i^\mu(t)$ in the thermodynamic limit. Furthermore, $r^\mu(t)$ is defined as

$$r^\mu(t) \equiv \lim_{N \rightarrow \infty} \frac{1}{A\sqrt{N}} \sum_{i \in \Lambda} \xi_i^\mu \sigma_i(t), \quad \mu \in \mathcal{P} \setminus \{1\}, \quad (17)$$

and $\tilde{r}^\mu(t)$ is given by a similar expression with $\sigma_i(t)$ replaced by $g_b(h_{\Lambda,i}(t) - \frac{1}{\sqrt{N}}\xi_i^\mu r_\Lambda^\mu(t))$. Finally, as can be read off from eq. (14) the quantity $M_i(t)$ consists out of a signal term and a discrete noise term, viz.

$$M_i(t) = \xi_i^1 m^1(t) + \alpha \chi(t-1) \sigma_i(t-1) + F \sum_{t'=0}^{t-2} \alpha \left[\prod_{s=t'}^{t-1} \chi(s) \right] \sigma_i(t'). \quad (18)$$

Since different architectures contain different correlations not all terms in these final equations are present, as is apparent through F . We remark that for the asymmetric diluted and the layered feedforward architecture $M_i(t) = \xi_i^1 m^1(t)$ so that in these cases the local field consists out of a signal term plus Gaussian noise for *all* time steps [6],[7].

For the architectures treated here we still have to determine the probability density $f_{h_i(t)}$ in eq. (16). This can be done by looking at the form of $M_i(t)$ given by eq. (18). The evolution equation tells us that $\sigma_i(t')$ can be replaced by $g_b(h_i(t'-1))$ such that the second and third terms of $M_i(t)$ are the sums of stepfunctions of correlated variables. These are also correlated through the dynamics with the normally distributed part of $h_i(t)$. Therefore, the local field can be considered as a transformation of a set of correlated normally distributed variables x_s , which we choose to normalize. Defining the correlation matrix $W = (\rho(s, s') \equiv \mathbb{E}[x_s x_{s'}])$ we arrive at the following expression for $f_{h_i(t)}$ for the fully connected model

$$\begin{aligned} f_{h_i(t)}(y) &= \int dx_t \prod_{s=0}^{t-2} dx_s \delta\left(y - M_i(t) - \sqrt{V(t)} x_t\right) \\ &\times \frac{1}{\sqrt{\det(2\pi W)}} \exp\left(-\frac{1}{2} \mathbf{x} W^{-1} \mathbf{x}^T\right) \end{aligned} \quad (19)$$

with $\mathbf{x} = \{x_s\} = (x_0, \dots, x_{t-2}, x_t)$. For the symmetric diluted case this expression simplifies to

$$\begin{aligned} f_{h_i(t)}(y) &= \int \prod_{s=0}^{[t/2]} dx_{t-2s} \delta\left(y - \xi_i^1 m^1(t) - \alpha \chi(t-1) \sigma_i(t-1) - \sqrt{\alpha a(t)} x_t\right) \\ &\times \frac{1}{\sqrt{\det(2\pi W)}} \exp\left(-\frac{1}{2} \mathbf{x} W^{-1} \mathbf{x}^T\right) \end{aligned} \quad (20)$$

with $\mathbf{x} = (\{x_s\}) = (x_{t-2[t/2]}, \dots, x_{t-2}, x_t)$. The brackets $[t/2]$ denote the integer part of $t/2$.

4 Gap structure

The equilibrium distribution of the local field can be obtained by eliminating the time dependence in the evolution equations (12)

$$h_i = \xi_i^1 m^1 + \eta \mathcal{N}(0, \alpha a) + \alpha \chi \eta \sigma_i \quad (21)$$

with $\eta = 1/(1-\chi)$ for the fully connected architecture and $\eta = 1$ for the extremely diluted one. The corresponding updating rule (4)

$$\sigma_i = g_b(\tilde{h}_i + \alpha \chi \eta \sigma_i), \quad \tilde{h}_i = \xi_i^1 m_i^1 + \eta \mathcal{N}(0, \alpha a) \quad (22)$$

in general admits more than one solution. A Maxwell construction (see, e.g., refs. [9],[10],[12]) can be made leading to a unique solution

$$\sigma_i = g_{\tilde{b}}(\tilde{h}_i), \quad \tilde{b} = (b - \frac{\alpha \eta \chi}{2}) \quad (23)$$

such that we have

$$\sigma_i = s_k \quad \text{if} \quad \tilde{b}(s_k + s_{k-1}) + \alpha \chi \eta s_k < h_i < \tilde{b}(s_k + s_{k+1}) + \alpha \chi \eta s_k. \quad (24)$$

for $\tilde{b} > 0$. This unique solution can be used to obtain fixed-point equations for the main overlap and activity (7). Those equations which we choose not to write down explicitly here (see refs. [9],[10]) are equal to the equations derived from a thermodynamic replica-symmetric mean-field theory approach [13],[14]. We remark that for analog networks ($Q \rightarrow \infty$) such a Maxwell construction is not necessary because eq. (22) has only one solution.

Next, we calculate the probability density of the local field by plugging this result (22)-(24) into (21) to obtain, forgetting about the site index i and the pattern index 1

$$f(h) = \sum_{k=1}^Q \frac{1}{\eta \sqrt{2\pi \alpha a}} \exp\left(-\frac{(h - \xi m - \alpha \chi \eta s_k)^2}{2\alpha a \eta^2}\right) \times \left(\theta[\tilde{b}(s_k + s_{k+1}) + \alpha \chi \eta s_k - h] - \theta[\tilde{b}(s_k + s_{k-1}) + \alpha \chi \eta s_k - h] \right) \quad (25)$$

meaning that (Q-1) gaps occur respectively at $\tilde{b}(s_k + s_{k-1}) + \alpha \chi \eta s_{k-1} < h < \tilde{b}(s_k + s_{k+1}) + \alpha \chi \eta s_k$ with width $\Delta h = 2\alpha \chi \eta / (Q - 1)$. For analog networks no gaps occur. When $\tilde{b} \leq 0$ the effective gain function (23) becomes two-state Ising-like as in the Hopfield model such that case only one gap occurs.

For $Q = 2$ this expression simplifies to

$$\begin{aligned}
f(h) &= \frac{1}{\eta\sqrt{2\pi\alpha a}} \exp\left(-\frac{(h - \xi m - \alpha\chi\eta)^2}{2\alpha a\eta^2}\right) \theta(h - \alpha\chi\eta) \\
&+ \frac{1}{\eta\sqrt{2\pi\alpha a}} \exp\left(-\frac{(h - \xi m + \alpha\chi\eta)^2}{2\alpha a\eta^2}\right) \theta(-h - \alpha\chi\eta)
\end{aligned} \tag{26}$$

and for $Q=3$ we have

$$\begin{aligned}
f(h) &= \frac{1}{\eta\sqrt{2\pi\alpha a}} \exp\left(-\frac{(h - \xi m - \alpha\chi\eta)^2}{2\alpha a\eta^2}\right) \theta(h - \tilde{b} - \alpha\chi\eta) \\
&+ \frac{1}{\eta\sqrt{2\pi\alpha a}} \exp\left(-\frac{(h - \xi m)^2}{2\alpha a\eta^2}\right) \theta(\tilde{b}^2 - h^2) \\
&+ \frac{1}{\eta\sqrt{2\pi\alpha a}} \exp\left(-\frac{(h - \xi m + \alpha\chi\eta)^2}{2\alpha a\eta^2}\right) \theta(-\tilde{b} - \alpha\chi\eta - h).
\end{aligned} \tag{27}$$

Similar formula can be written down for bigger values of Q . For $Q = 2$ this result seems to be consistent with the gap in the internal-field distribution for an infinite range spin glass found by a Bethe-Peierls-Weiss approach [15] (see also [16]-[17]).

We have investigated this probability distribution numerically using the corresponding fixed-point equations mentioned before, for several values of Q and compared them with those obtained from numerical simulations of the dynamics for networks of $N = 6000$ neurons. Some typical results are shown in figs. 1-6.

In figs. 1-2 the local field distribution for the fully connected $Q = 2$ network is shown for a retrieval state ($\alpha = 0.13, m_0 = 0.5$) just below the critical capacity and a non-retrieval spin-glass state ($\alpha = 0.14, m_0 = 0.2$) just above it. Both the first few time steps and the equilibrium result derived above are compared with numerical simulations. They are in agreement. For the retrieval state there is, typically, a small gap in the equilibrium distribution around $h=0$. For small α the gap is very narrow. Furthermore, in the simulations one sees that this gap shows up very quickly. For the non-retrieval state the gap is typically much bigger. Again in the simulations one quickly sees the gap but it is extremely difficult numerically to find points touching the zero axis because of finite size effects.

Figure 3 shows the gap width at equilibrium, Δh , for the non-retrieval state as a function of Q with $b = 0.5$. It scales as $\Delta h \sim 1/(Q-1)$ and, hence, decreases to zero for $Q \rightarrow \infty$. This constant behaviour of $(Q-1)\Delta h$ attains already for values of $Q \geq 20$ and is also seen for the retrieval state. These results are insensitive to the structure of the symmetric architecture.

In figure 4 the gap boundaries in h as a function of α are compared for retrieval and non-retrieval states in the symmetric diluted $Q = 3, b = 0.2$ model. We remark that in this case the spin-glass states do not exist for $\alpha \leq 0.04$ [14] so that there is no gap for these α -values. For α large enough ($\alpha > 0.465$ for retrieval states and $\alpha > 0.252$ for spin-glass states) there exists one gap only since the effective gain function becomes Ising-like [14]. More gaps with smaller widths are formed when increasing Q for both the fully connected and diluted models. For $Q \rightarrow \infty$ the gaps disappear.

Figure 5 compares the gaps for the spin-glass states in the fully connected and symmetric diluted $Q = 3$ models with $b = 0.5$. For $\alpha \leq 0.25$ there exist no spin-glass states in the diluted model [14] and for $\alpha \leq 0.004$ there are none in the fully connected model [13]. When both do exist the gap widths are almost equal. So the dilution has some influence on the existence of the gap but, again, not on its width.

Finally, fig. 6 presents the local field distribution for the symmetric diluted $Q = 3, b = 0.5$ model for a retrieval state ($\alpha = 0.6, m_0 = 0.7$) just below the critical capacity. Only the distribution with pattern values +1 is shown. It is asymmetric and two gaps are found at equilibrium. For pattern values 0 the distribution is symmetric and the gap locations and widths are the same (see eq. (25)) but their height is different.

In conclusion, we have studied the time evolution of the local field in symmetric Q -Ising neural networks both in the retrieval and spin-glass regime. We have found a gap structure in the local field distribution depending on the specific architecture and on the value of Q . The results agree with the numerical simulations we have performed.

Acknowledgments

This work has been supported in part by the Fund of Scientific Research, Flanders-Belgium and the Korea Science and Engineering Foundation through the SRC program. The authors are indebted to A. Coolen, G. Jongen and V. Zagrebnoy for constructive discussions.

References

- [1] A.E. Patrick and V.A. Zagrebnoy, Parallel dynamics for an extremely diluted neural network, *J. Phys. A: Math. Gen.* **23**: L1323 (1990); *J. Phys. A: Math.*

- Gen.* **25**: 1009 (1992).
- [2] A.E. Patrick and V.A. Zagrebnoy, On the parallel dynamics for the Little-Hopfield model, *J. Stat. Phys.* **63**: 59 (1991).
 - [3] T.L.H. Watkin and D. Sherrington, The parallel dynamics of a dilute symmetric neural network, *J. Phys. A: Math. Gen.* **24**: 5427 (1991).
 - [4] A.E. Patrick and V.A. Zagrebnoy, A probabilistic approach to parallel dynamics for the Little-Hopfield model, *J. Phys. A: Math. Gen.* **24**: 3413 (1991).
 - [5] D. Bollé, B. Vinck, and V.A. Zagrebnoy, On the parallel dynamics of the Q -state Potts and Q -Ising neural networks, *J. Stat. Phys.* **70**: 1099 (1993).
 - [6] D. Bollé, G.M. Shim, B. Vinck, and V.A. Zagrebnoy, Retrieval and chaos in extremely diluted Q -Ising neural networks, *J. Stat. Phys.* **74**: 565 (1994).
 - [7] D. Bollé, G.M. Shim, and B. Vinck, Retrieval and chaos in layered Q -Ising neural networks, *J. Stat. Phys.* **74**: 583 (1994).
 - [8] D. Gandolfo, M. Sirugue-Collin and V.A. Zagrebnoy, Local instability and oscillations of trajectories in a diluted symmetric neural network, *Network: Computation in Neural Systems* **9**: 563 (1998)
 - [9] D. Bollé, G. Jongen and G.M. Shim, Parallel dynamics of fully connected Q -Ising neural networks, *J. Stat. Phys.* **91**: 125 (1998).
 - [10] D. Bollé, G. Jongen and G.M. Shim, Parallel dynamics of extremely diluted symmetric Q -Ising neural networks, *J. Stat. Phys.* **96**: 861 (1999).
 - [11] A.N. Shiriyayev, *Probability* (Springer, New York, 1984).
 - [12] M. Shiino and T. Fukai, Self-consistent signal-to-noise analysis of the statistical behavior of analog neural networks and enhancement of the storage capacity, *Phys. Rev. E* **48**: 867 (1993).
 - [13] D. Bollé, H. Rieger and G.M. Shim, Thermodynamic properties of fully connected Q -Ising neural networks, *J. Phys. A: Math. Gen.* **27**: 3411 (1994).
 - [14] D. Bollé, D. Carlucci and G.M. Shim, Thermodynamic properties of extremely diluted Q -Ising neural networks, *J. Phys. A: Math. Gen.* **33**: 6481 (2000).
 - [15] L.J. Schowalter and M.W. Klein, Analytic treatment of the hole in the internal field distribution for an infinite-range spin glass, *J.Phys.C: Solid State Physics* **12**: L935 (1979).

- [16] V.A. Zagrebnov and A.S. Chvyrov, The Little-Hopfield model: recurrence relations for retrieval-pattern errors, *Sov.Phys.JETP* **68**: 153 (1989)
- [17] A.C.C. Coolen and D. Sherrington, Order parameter flow in the fully connected Hopfield model near saturation, *Phys. Rev. E* **49**: 1921 (1994).

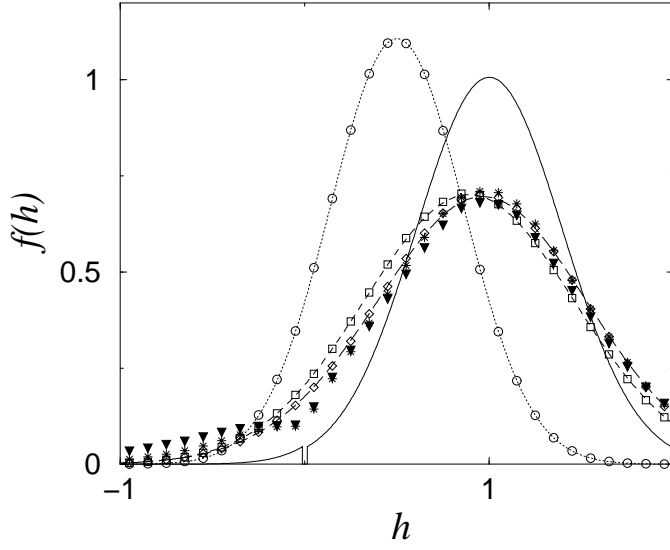


Figure 1: A comparison of theoretical results and numerical simulations with $N = 6000$ for the local field distribution $f(h)$ of a retrieval state in the $Q = 2$ system with network parameters $\alpha = 0.13, m_0 = 0.5$. Theoretical (simulation) results for time step $t = 0, 1, 2$ are indicated by a dotted curve (circles), a short-dashed curve (squares) and a long-dashed curve (diamonds). Simulations for $t = 10, 20$ (stars, triangles) are shown and the full curve presents the equilibrium distribution.

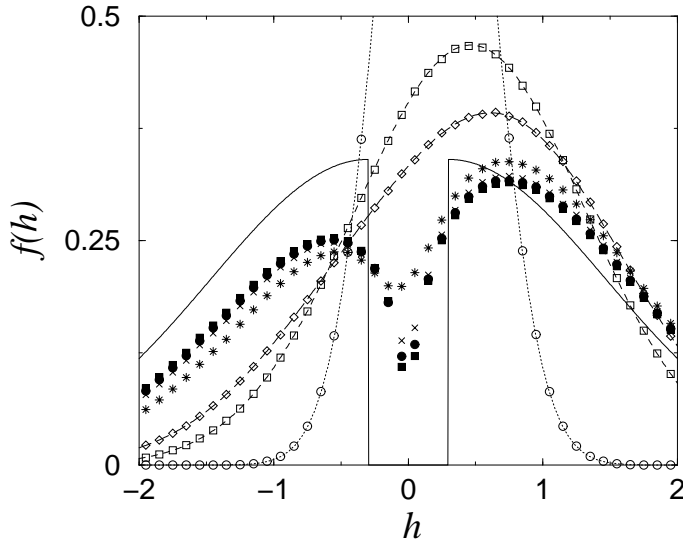


Figure 2: As in Fig. 1, for a $Q = 2$ non-retrieval spin-glass state with the network parameters $\alpha = 0.14, m_0 = 0.2$. Further simulations for $t = 10$ (stars), $t = 30$ (crosses), $t = 50$ (filled circles) and $t = 100$ (filled squares) are shown.

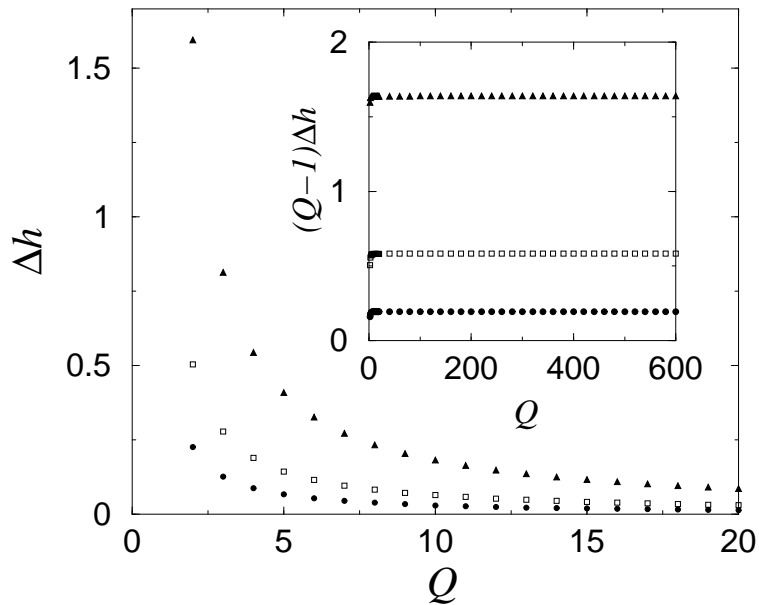


Figure 3: The gap width Δh for non-retrieval states as a function of Q for the gain parameter $b = 0.5$ for $\alpha = 1$ (triangles), $\alpha = 0.1$ (squares) and $\alpha = 0.01$ (filled circles). The inset details the corresponding scaling properties.

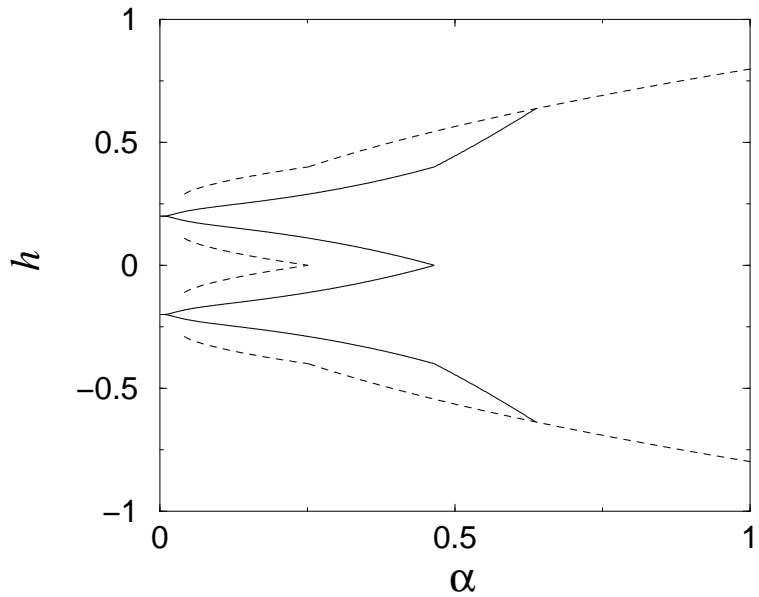


Figure 4: The gap boundaries in h as a function of α for retrieval (full curve) and non-retrieval (dashed curve) states for the $Q = 3$ symmetric diluted systems with gain parameter $b = 0.2$.

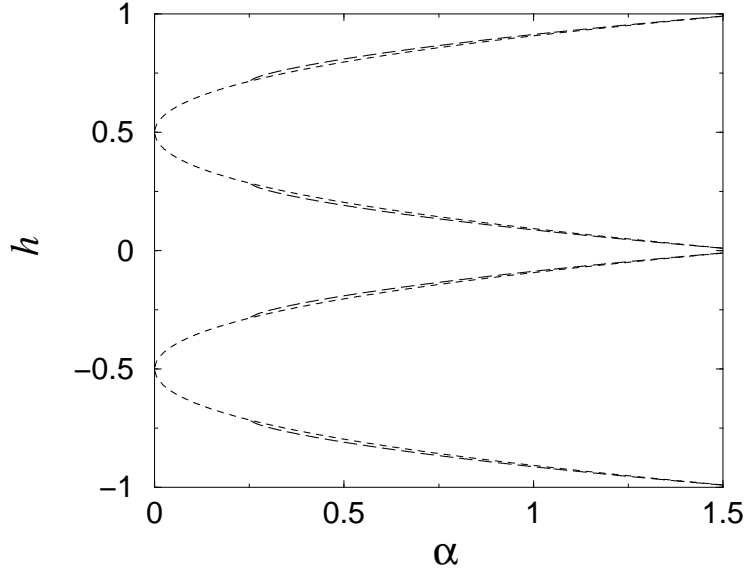


Figure 5: The gap boundaries in h as a function of α for spin-glass states in the fully connected (short-dashed curve) and symmetric diluted (long-dashed curve) $Q = 3$ system with gain parameter $b = 0.5$.

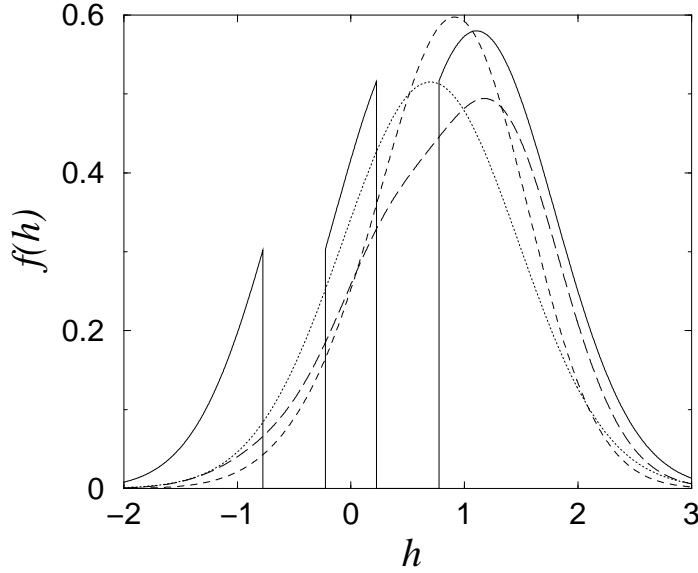


Figure 6: The local field distribution $f(h)$ of a retrieval state for pattern values $+1$ in the symmetric diluted $Q = 3$ system with network parameters $\alpha = 0.6, b = 0.5, m_0 = 0.7$. Results for $t = 0, 1, 2, \infty$ are indicated by a dotted curve, a short-dashed curve, a long-dashed curve and a full curve respectively.